1979

A structural analysis of the water protons in a single crystal of Er(C(2)H(5)SO(4))(3).9H(2)O by NMR.

Setsuko. Sato
University of Windsor

NOTICE

The quality of this microfiche is heavily dependent upon the quality of the original thesis submitted for microfilming. Every effort has been made to ensure the highest quality of reproduction possible.

If pages are missing, contact the university which granted the degree.

Some pages may have indistinct print especially if the original pages were typed with a poor typewriter ribbon or if the university sent us a poor photocopy.

Previously copyrighted materials (journal articles, published tests, etc.) are not filmed.

Reproduction in full or in part of this film is governed by the Canadian Copyright Act, R.S.C. 1970, c. C-30. Please read the authorization forms which accompany this thesis.

THIS DISSERTATION
HAS BEEN MICROFILMED
EXACTLY AS RECEIVED

AVIS

La qualité de cette microfiche dépend grandement de la qualité de la thèse soumise au microfilmage. Nous avons tout fait pour assurer une qualité supérieure de reproduction.

S'il manque des pages, veuillez communiquer avec l'université qui a conféré le grade.

La qualité d'impression de certaines pages peut laisser à désirer, surtout si les pages originales ont été dactylographiées à l'aide d'un ruban usé ou si l'université nous a fait parvenir une photocopie de mauvaise qualité.

Les documents qui font déjà l'objet d'un droit d'auteur (articles de revue, examens publiés, etc.) ne sont pas microfilmés.

La reproduction, même partielle, de ce microfilm est soumise à la Loi canadienne sur le droit d'auteur, SRC 1970, c. C-30. Veuillez prendre connaissance des formules d'autorisation qui accompagnent cette thèse.

LA THÈSE A ÉTÉ
MICROFILMÉE TELLE QUE
NOUS L'AVONS REÇUE

A STRUCTURAL ANALYSIS OF THE WATER PROTONS IN A SINGLE CRYSTAL OF $Er(C_2H_5SO_4)_3 \cdot 9H_2O$ BY NMR

BY

SETSUKO SATO

A Thesis

Submitted to the Faculty of Graduate Studies through the Department of Chemistry in Partial Fulfillment of the Requirements for the Degree of Master of Science at the University of Windsor

Windsor, Ontario

1979

APPROVED BY:

Bruce R. McTaggart

Robert C. Rumfeldt

al J. Clerizo

To My Parents

ABSTRACT

The structure of the water protons in a single crystal of the erbium ethylsulfate $\cdot 9H_2O$ has been studied by nuclear magnetic resonance. The proton resonances of this crystal are shifted from the usual bulk proton NMR by the interaction with the unpaired electrons in the Er^{+3} ion. The crystal was rotated in three orthogonal planes in the magnetic field and the variations of the shift in the three rotational planes gave the shift tensor which depends on the orientation of a proton in the crystal. For the experimental temperatures between -22.5° and $-28.5^{\circ}C$ only one pair of lines split by the nuclear-nuclear dipolar interaction was observed for each water molecule. The two protons in the water molecule should have different shift tensors but some motional process averages them at these temperatures. Therefore one pair of shift tensors was obtained for each water molecule. The principal values of the shift tensors were obtained by the diagonalization of the shift tensor for each symmetrically equivalent water site. These principal values of the experimental shift tensors were compared with the principal values of shift tensors which were calculated from the predicted hydrogen positions by the point dipole model and the magnetic susceptibility of $Er(C_2H_5SO_4)_3 \cdot 9H_2O$. The hydrogen coordinates were changed until the best fit of the computed principal values with the experimental values was obtained and the hydrogen positions giving the best agreement are reported.

TABLE OF CONTENTS

LIST OF FIGURES

Chapter 1

INTRODUCTION

A. Previous Studies of Rare-Earth Ethylsulfate · $9H_2O$.

The structure of rare-earth ethylsulfate · $9H_2O$ has been studied by several techniques. X-ray diffraction was first used by Ketelaar[1] (1937). Fitzwater and Rundle[2] (1959) did a more accurate study, especially for the Er and Pr compounds. It is hard to determine hydrogen positions from X-ray diffraction and Ketelaar, Fitzwater, and Rundle determined the positions of all atoms except hydrogens. Albertsson and Elding[3] (1976) investigated the Yb and Pr compounds by X-ray and tried to estimate hydrogen positions. Neutron diffraction is a more powerful method for determing hydrogen than X-ray diffraction. Hubbard, Quicksall and Jacobson[4] (1974) used this technique to investigate the Ho compound.

The NMR technique is completely different from the diffraction method. The application of this technique to an analysis of structure was first tried by Pake[5] (1947) in the study of $CaSO_4 \cdot 2H_2O$. Wolfe, et al.[6,7] (1972,1977) used the NMR method to determine the structure of water protons near rare earth ions doped into a crystal of yttrium ethylsulfate · $9H_2O$.

B. Nuclear Magnetic Resonance

All nuclei except even-even nuclei possess the property of spin. In the case of a proton the value of the spin, I, is 1/2 and the magnetic moment associated with this spin can be oriented in the magnetic field with the component of the magnetic moment along the

field direction having only values of $\frac{1}{2}g_N\beta_N$ or $-\frac{1}{2}g_N\beta_N$. These magnetic moments interact with the external magnetic field. Protons which have a magnetic moment of $-\frac{1}{2}g_N\beta_N$ have higher energy than those which have a magnetic moment of $\frac{1}{2}g_N\beta_N$.

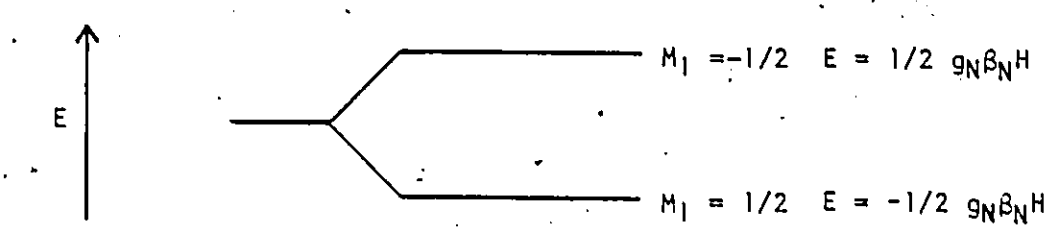

Fig. 1 Proton Spin Levels In a Magnetic Field

The distribution of protons, that is how many protons in the higher state or the lower state, is dependent on the temperature and is found from Boltzmann's equation at equilibrium, although it takes some time to reach the equilibrium. At room temperature the population of the lower state is slightly larger than that of the higher state.

When a photon is added to protons and the frequency satisfies the following equation, the energy is absorbed and a stimulated transition between these two levels occurs.

$$\Delta E = h\nu = g_N\beta_N H \qquad \{1\}$$

There are two ways to detect this transition energy: one of them is that at a fixed magnetic field the radiofrequency is changed and another is that at a fixed radiofrequency the magnetic field is changed. In this work the latter way was used.

C. The NMR Measurement of Rare-Earth Ethylsulfate at Low Temperature

For rare-earth compounds the crystal field is weak compared with the spin-orbit coupling, because unpaired electrons are in an inner shell and are well shielded from the crystal field.

Trivalent ytterbium ($4f^{13}$, $^2F_{7/2}$ ground multiplet) which Wolfe et al.[6,7] studied with NMR at <4.2°K in yttrium ethylsulfate is a Kramers ion and it is known that $J_z = \pm 3/2$ doublet lies lowest from far-infrared optical measurements[8], with the first excited doublet being $J_z = \pm 1/2$ at 44 cm^{-1}. These Kramers doublets split in the magnetic field, as shown in Fig. 2. At <4.2°K only the lowest lying state is populated. Wolfe, et al. found that at external magnetic fields <20 kG, admixtures from excited states into the ground state is very small and the resulting second-order Zeeman correction to the NNMR splittings was less than 3G over the given field range. Under this condition, the NMR experiments by Wolfe, et. al. may be explained by introducing the effective spin Hamiltonian with S = 1/2, which is given by

$$H_S = \beta \vec{S} \cdot g \cdot \vec{H} - g_N \beta_N \vec{H} \cdot \vec{I} + h \vec{S} \cdot A \cdot \vec{I} \qquad \{2\}$$

The concept of this spin Hamiltonian was first advanced and developed by Abragam and Pryce.[9,10] Each state of $J_z = 3/2$ and $J_z = -3/2$ which are split in the magnetic field still has a net orbital moment so that S_z is not purely 1/2 or -1/2. However this state behaves like a pure spin state, with a g value different from that of the free electron. Eq. (2) was developed experimentally and gives a satisfactory fit with theoretical calculations.

Then the energy diagram may be written as Fig. 3. For the diagram in Fig. 3, splitting is caused by electron Zeeman interaction,

Figure 2

Splitting of the states of a $4f^{13}$ ion by the combined action of spin-orbit coupling, a trigonal crystal field, and an external magnetic field.

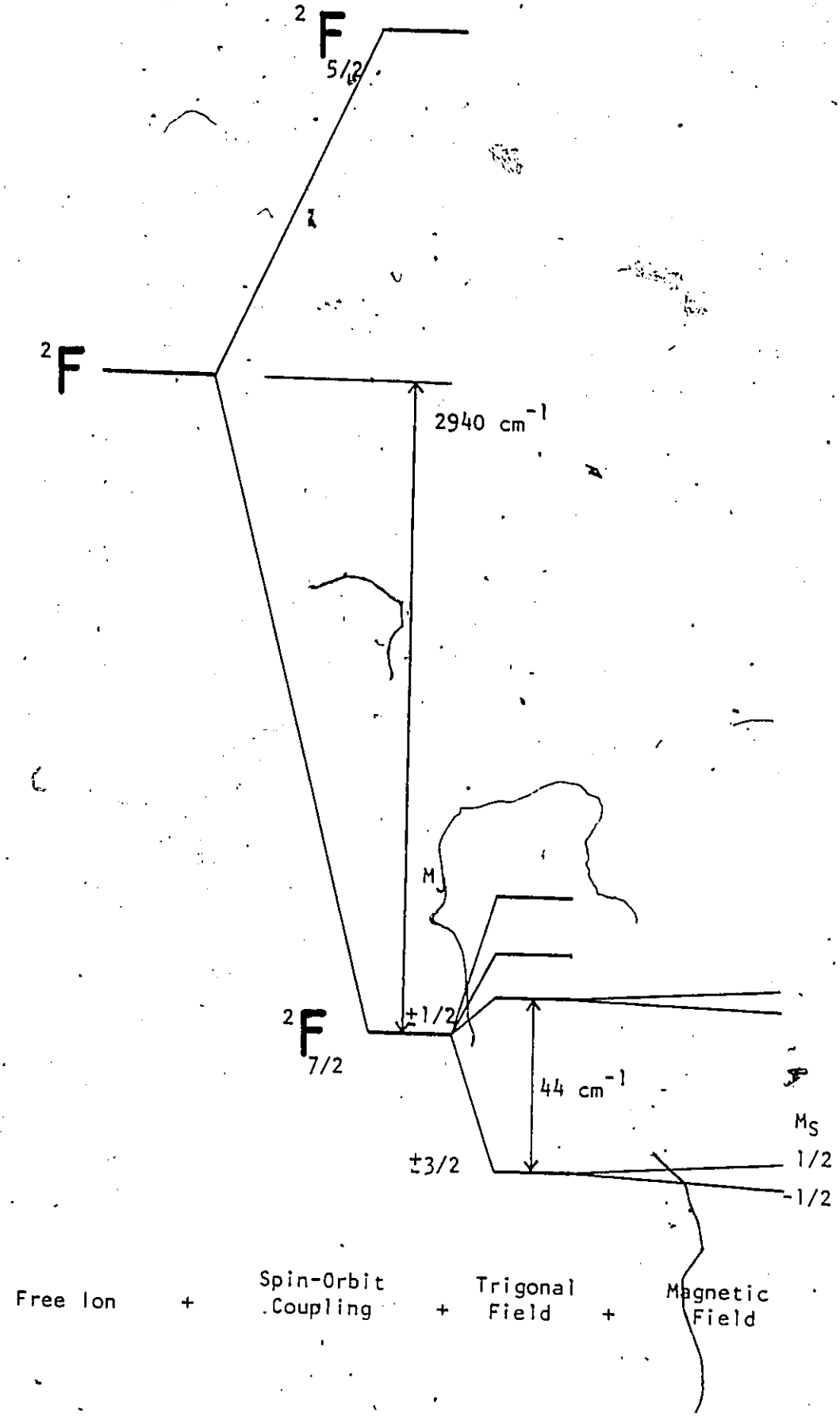
$^2F_{5/2}$
^2F
2940 cm^{-1}
M
$^2F_{7/2}$
±1/2
44 cm^{-1}
M_S
±3/2
1/2
-1/2
Free Ion + Spin-Orbit Coupling + Trigonal Field + Magnetic Field

Figure 3

Energy diagram for effective electron spin, S = 1/2 and nuclear spin, I = 1/2.

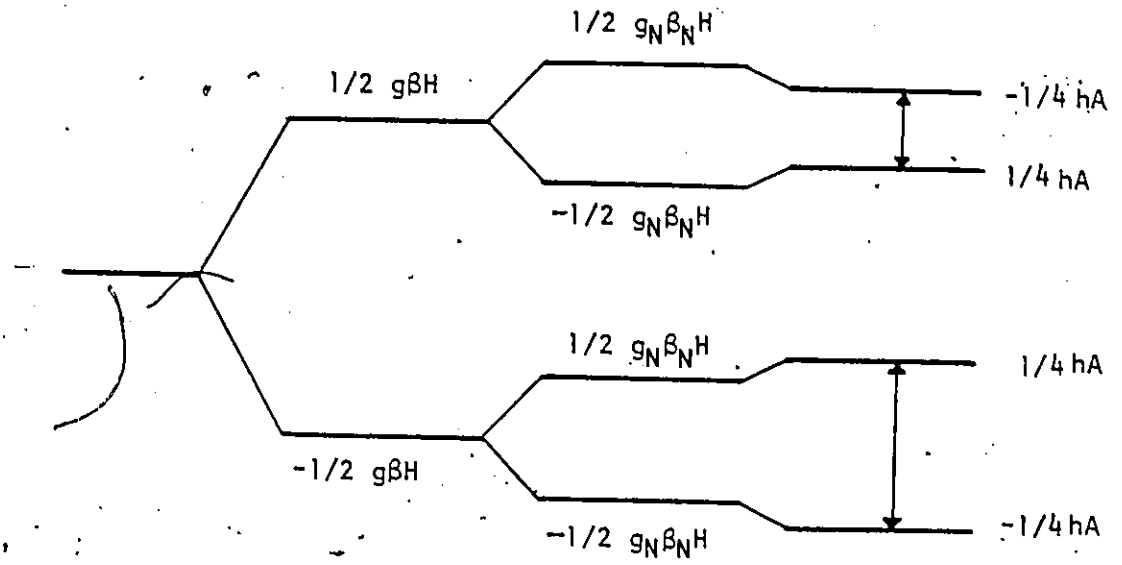

Free Ion	+ Electron Zeeman Interaction	+ Nuclear Zeeman Interaction	+ Hyperfine Interaction

nuclear Zeeman interaction and the hyperfine interaction between unpaired electrons in the rare-earth ion and nuclear spin of protons in the magnetic field. The allowed NMR transitions occur between the levels which are shown by arrows in the diagram. The differences of energy are given by

$$\Delta E = g_N \beta_N H \pm 1/2\, hA \qquad \{3\}$$

In the NMR measurements made by Wolfe, et al. both transitions shown in Fig. 3 were observed and measured. To do this it is essential that the spin-lattice relaxation time be very long for the electronic spin states of the rare-earth ion. For this reason very low temperatures were required to make the measurements. In addition, it was necessary to make measurements on systems in which the rare-earth ions were far apart, because impurity rare-earth ions which are close to each other interact with each other and these spins flip mutually. This makes the spin-lattice relaxation time shorter. Also, at very low temperatures such as $<4.2^{o}K$, one hydrogen nucleus can distinguish the neighbors which have spin 1/2 or -1/2. The distribution of 1/2 or -1/2 on neighbors is random so that these neighbors give an unordered local field at the proton whose NMR is being studied. This makes absorption lines broad.

Effective S in Eq. (2) is not quantized along the external field direction due to the anisotropy of g factor, which is caused by the remaining orbital moment.

The hyperfine interaction term of Eq. (2) is primarily due to the dipolar interaction which is given by

$$H_D = \frac{\vec{\mu}_e \cdot \vec{\mu}_N}{r^3} - \frac{3(\vec{\mu}_e \cdot \vec{r})(\vec{\mu}_N \cdot \vec{r})}{r^5} \qquad \{4\}$$

where $\vec{\mu}_e$ and $\vec{\mu}_N$ are the electron and nuclear magnetic moments, $\vec{r}$ is the vector joining an electron and a nucleus and r is a distance between them. For an anisotropic g factor the electron magnetic moment is given by

$$\vec{\mu}_e = \beta\{S_x g_\perp, S_y g_\perp, S_z g_\parallel\} \qquad \{5\}$$

Also the nuclear magnetic moment is

$$\vec{\mu}_N = g_N \beta_N \vec{I} = g_N \beta_N \{I_x, I_y, I_z\} \qquad \{6\}$$

Using these magnetic moments Eq. (4) gives

$$H_D = \frac{g_N \beta_N \beta}{r^5} \left[S_x g_\perp, S_y g_\perp, S_z g_\parallel \right] \cdot \begin{bmatrix} r^2-3x^2 & -3xy & -3zx \\ -3xy & r^2-3y^2 & -3yz \\ -3zx & -3yz & r^2-3z^2 \end{bmatrix} \cdot \begin{bmatrix} I_x \\ I_y \\ I_z \end{bmatrix} \qquad \{7\}$$

Wolfe's technique is of great advantage for Kramers ion with high quality instruments, but it cannot be applied to a study of a single crystal of a pure rare-earth ethylsulfate $\cdot 9H_2O$ and at higher temperatures. At higher temperatures the spin relaxation time is very short so that electron spins change very rapidly. As a result one can observe only a time-averaged hyperfine interacion that is an admixture of two energy differences. We are interested in the analysis of positions of water hydrogens in a single crystal of erbium ethylsulfate $\cdot 9H_2O$ so that the time-averaged hyperfine interaction is studied.

D. Time Averaged Hyperfine Interaction of Er Ethylsulfate $\cdot 9H_2O$

Trivalent erbium ($4f^{11}$, $^4I_{15/2}$ ground multiplet) has three unpaired electrons. Although for the ground state J_z can be $\pm$ 15/2, $\pm$13/2, $\pm$11/2 and $\pm$9/2, at higher temperatures other states are also populated. Due to a very short spin lattice relaxation time at room

temperature rare-earth ions change states so rapidly that the spin and orbital moment is averaged over all thermally populated states.

The equation for the hyperfine interaction of the nuclear spin with the electron's spin and orbital motion can be obtained by following Kurland and McGarvey's[11,12] calculation in which perturbation theory was used in a manner similar to what Van Vleck[13] did for magnetic susceptibilities. The hyperfine interaction which was obtained by averaging over all thermally populated states is simply expressed as

$$H_{Hyp.} = \vec{H} \cdot A \cdot \vec{I} \qquad \{8\}$$

where A is given by

$$A_{ij} = q^{-1} \sum_n \left\{ - \frac{\langle \Phi_n | \beta(L_i + g_e S_i) | \Phi_n \rangle \langle \Phi_n | H_{Nj} | \Phi_n \rangle}{kT} \right.$$

$$+ \sum_m \left(\frac{\langle \Phi_n | \beta(L_i + g_e S_i) | \Phi_m \rangle \langle \Phi_m | H_{Nj} | \Phi_n \rangle}{E_n - E_m} \right.$$

$$\left. \left. + \frac{\langle \Phi_n | H_{Nj} | \Phi_m \rangle \langle \Phi_m | \beta(L_i + g_e S_i) | \Phi_n \rangle}{E_n - E_m} \right) \right\} \exp\left(\frac{E_n}{kT}\right) \qquad \{9\}$$

where E_n and Φ_n are energy and eigenfunction in the absence of a magnetic field, where n is the index denoting the eigenstate, and g_e is free electron g value. Then the spin Hamiltonian for a nearby nuclear spin is written as

$$H_S = -g_N \beta_N \vec{H} \cdot \vec{I} + \vec{H} \cdot A \cdot \vec{I}$$

$$= -g_N \beta_N \vec{H} \cdot (1 - a) \cdot \vec{I} \qquad \{10\}$$

where $a = \frac{1}{g_N \beta_N} A$

The secular determinant for I = 1/2 gives the following solution.

$$E^2 = 1/4\, g_N^2\beta_N^2 \Big[H_z^2\{(1-a_{zz})^2 + a_{zx}^2 + a_{zy}^2\} + H_x^2\{(1-a_{xx})^2 + a_{xz}^2 + a_{xy}^2\}$$
$$+ H_y^2\{(1-a_{yy})^2 + a_{yz}^2 + a_{yx}^2\}$$
$$+ H_xH_y\{-2a_{xz}a_{yz} - 2a_{yx}(1-a_{xx}) - 2a_{xy}(1-a_{yy})\}$$
$$+ H_xH_z\{-2a_{xz}(1-a_{zz}) - 2a_{zx}(1-a_{xx}) - 2a_{xy}a_{zy}\}$$
$$+ H_yH_z\{-2a_{yz}(1-a_{zz}) - 2a_{yx}a_{zx} - 2a_{zy}(1-a_{yy})\} \Big] \qquad \{11\}$$

The equation may be written as

$$E^2 = 1/4\, g_N^2\beta_N^2 \vec{H}\cdot G^2\cdot\vec{H} \qquad \{12\}$$

where
$$G_{zz}^2 = (1-a_{zz})^2 + a_{zx}^2 + a_{zy}^2$$
$$G_{xz}^2 = G_{zx}^2 = -a_{xz}(1-a_{zz}) - a_{zx}(1-a_{xx}) - a_{xy}a_{zy}$$
$$G_{yz}^2 = G_{zy}^2 = -a_{yz}(1-a_{zz}) - a_{yx}a_{zy} - a_{zy}(1-a_{yy})$$
$$G_{yy}^2 = (1-a_{yy})^2 + a_{yz}^2 + a_{yx}^2$$
$$G_{xx}^2 = (1-a_{xx})^2 + a_{xz}^2 + a_{xy}^2$$
$$G_{xy}^2 = G_{yx}^2 = -a_{xz}a_{yz} - a_{yx}(1-a_{xx}) - a_{xy}(1-a_{yy})$$

When $a \ll 1$

$$G_{zz}^2 \simeq 1-2a_{zz}, \qquad G_{xx}^2 \simeq 1-2a_{xx} \qquad G_{yy}^2 \simeq 1-2a_{yy}$$
$$G_{xz}^2 \simeq -a_{xz}-a_{zx} \qquad G_{xy}^2 \simeq -a_{yx}-a_{xy} \qquad G_{yz}^2 \simeq -a_{yz}-a_{zy}$$

Therefore Eq. (11) can be given approximately as follows:

$$E^2 \simeq 1/4\, g_N^2\beta_N^2 \Big\{ H_x^2 + H_y^2 + H_z^2 - 2a_{zz}H_z^2 - 2a_{xx}H_x^2 - 2a_{yy}H_y^2$$
$$- 2(a_{xz}+a_{zx})H_xH_z - 2(a_{xy}+a_{yx})H_xH_y - 2(a_{yz}+a_{zy})H_yH_z \Big\}$$
$$\simeq 1/4\, g_N^2\beta_N^2 \Big[H - H\{a_{zz}\frac{H_z^2}{H^2} + a_{xx}\frac{H_x^2}{H^2} + a_{yy}\frac{H_y^2}{H^2}$$
$$+ (a_{xz}+a_{zx})\frac{H_xH_z}{H^2} + (a_{xy}+a_{yx})\frac{H_xH_y}{H^2} + (a_{yz}+a_{zy})\frac{H_zH_y}{H^2}\} \Big]^2$$

$$= 1/4\ g_N^2\beta_N^2H^2\left\{1-\frac{\vec{H}}{H}\cdot\begin{bmatrix} a_{xx} & \frac{1}{2}(a_{xy}+a_{yx}) & \frac{1}{2}(a_{xz}+a_{zx}) \\ \frac{1}{2}(a_{xy}+a_{yx}) & a_{yy} & \frac{1}{2}(a_{yz}+a_{zy}) \\ \frac{1}{2}(a_{xz}+a_{zx}) & \frac{1}{2}(a_{yz}+a_{zy}) & a_{zz} \end{bmatrix}\cdot\frac{\vec{H}}{H}\right\}^2 \quad \{13\}$$

where $H^2 = |\vec{H}|^2 = H_x^2 + H_y^2 + H_z^2$

when the matrix is expressed as $\bar{a}$, and $\frac{\vec{H}}{H}$ is given as $\vec{h}_0$ which is a unit vector in the field direction, Eq. (13) is written as

$$E^2 = 1/4\ g_N^2\beta_N^2H^2\ \{1-\vec{h}_0\cdot\bar{a}\cdot\vec{h}_0\}^2 \quad \{14\}$$

Therefore

$$E = \pm 1/2\ g_N\beta_N H\ \{1-\vec{h}_0\cdot\bar{a}\cdot\vec{h}_0\} \quad \{15\}$$

The energy difference is given by

$$\Delta E = h\nu = g_N\beta_N H\ \{1-\vec{h}_0\cdot\bar{a}\cdot\vec{h}_0\} \quad \{16\}$$

At the fixed radiofrequency, ν_0

$$h\nu_0 = g_N\beta_N H_0 = g_N\beta_N H\ \{1-\vec{h}_0\cdot\bar{a}\cdot\vec{h}_0\} \quad \{17\}$$

Therefore $\frac{\Delta H}{H_0} = \frac{\vec{h}_0\cdot\bar{a}\cdot\vec{h}_0}{1-\vec{h}_0\cdot a\cdot\vec{h}_0} \simeq \vec{h}_0\cdot\bar{a}\cdot\vec{h}_0$ $\{18\}$

$(\because a \ll 1)$

In this work the symmetrical tensor $\bar{a}$ is what is measured and reported.

E. Point Dipole Model Using Magnetic Susceptibility

As described in I-C, the electron spin moment with orbital moment is averaged and it is expressed simply as a dipole moment quantized along the magnetic field H_0. If there are no covalent or overlap interactions then the shift tensor of Eq. (18) can be related with the magnetization of the crystal and its susceptibility.

The rare-earth ion with this averaged moment can be considered as a point dipole with a magnetic moment of

$$\vec{\mu} = \chi . H \qquad \{19\}$$

where χ is the atomic susceptibility.

Reuveni and McGarvey[14] derived the equation which gives the hyperfine shift tensor calculated by this point dipole model using Eq. (4). This is given as

$$\left(\frac{\Delta H}{H_0}\right)_{ij} = \sum_k R_k^{-3} \left[3 \cos \Theta_i^k \left(\sum_l \chi_{lj}^k \cos \theta_l^k\right) - \chi_{ij}^k \right] \qquad \{20\}$$

where χ_{ij}^k is the susceptibility tensor component for the kth rare-earth ion, $\cos \Theta_i^k$ is the direction cosine of the ith vector coordinate of ion k, and R_k is the distance from the proton to the kth rare-earth ion.

The shift tensor for Er ethylsulfate $\cdot 9H_2O$ and other rare-earth ethylsulfates were calculated using Eq. (20) from the predicted hydrogen positions.

F. Nuclear-Nuclear Dipolar Interaction Between Protons in One Water Molecule

Fine structure in protons was first observed by G. E. Pake[5] in $CaSO_4 \cdot 2H_2O$.

While one proton's nuclear spin interacts with unpaired spins of rare-earth ions, it also interacts with the nuclear spin of the other hydrogen in the same water molecule. This nuclear-nuclear dipolar interaction also can be expressed in the same way as the electron-nuclear hyperfine interaction such as Eq. (7). In the case of the electron-nuclear hyperfine interaction, one magnet is an electron spin and another magnet is a nuclear spin, but here both magnets are nuclear spins.

Eq. (4) gives the nuclear-nuclear dipolar interaction terms as

$$H_D = \frac{g_N^2\beta_N^2}{r^5}\begin{bmatrix} I_{1x}, & I_{1y}, & I_{1z}\end{bmatrix}\cdot\begin{bmatrix} r^2-3x^2 & -3xy & -3xz \\ -3xy & r^2-3y^2 & -3yz \\ -3xz & -3yz & r^2-3z^2\end{bmatrix}\cdot\begin{bmatrix} I_{2x} \\ I_{2y} \\ I_{2z}\end{bmatrix} \quad \{21\}$$

where r is the distance between two protons. By using shift operator I^+ and I^- and polar coordinate system the main contribution of Eq. (21) is written as

$$H_D = g_N^2\beta_N^2 \frac{(1-3\cos^2\Theta)}{r^3}\{I_{1z}\, I_{2z} - 1/4(I_1^+I_2^- + I_1^-I_2^+)\} \quad \{22\}$$

Four energy states are

$$\begin{aligned} |t_1\rangle &= |\alpha_1\alpha_2\rangle \\ |t_0\rangle &= \frac{1}{\sqrt{2}}|\alpha_1\beta_2 + \beta_1\alpha_2\rangle \\ |t_{-1}\rangle &= |\beta_1\beta_2\rangle \\ |S\rangle &= \frac{1}{\sqrt{2}}|\alpha_1\beta_2 - \beta_1\alpha_2\rangle \end{aligned} \quad \{23\}$$

The calculation of Eq. (22) for these energy states gives the shift which is shown as follows

$$H = H' \pm 3/4\, g_N\beta_N\,(1-3\cos^2\Theta)/r^3 \quad \{24\}$$

Pake used the following equation

$$H = H^* \pm \alpha\{3\cos^2\delta\cos^2(\Phi-\Phi_0)-1\} \quad \{25\}$$

where $H^* = h\nu/2\mu$ is the resonance field for magnetic moment, μ, an applied radiofrequency ν and δ, Φ_0 and Φ are shown in Fig. 4. α is defined by the distance between hydrogens in a water molecule.

Wolfe, et al. obtained the near-proton NMR spectrum for Yb in yttrium ethylsulfate $\cdot 9H_2O$ along the c axis and observed pairs of lines due to the nuclear-nuclear dipolar interaction. From the separation of those lines he estimated a proton-proton distance of 1.56±0.01 A.

The nuclear-nuclear dipolar interaction tensors for predicted positions calculated from the structure, were obtained using Eq. (25).

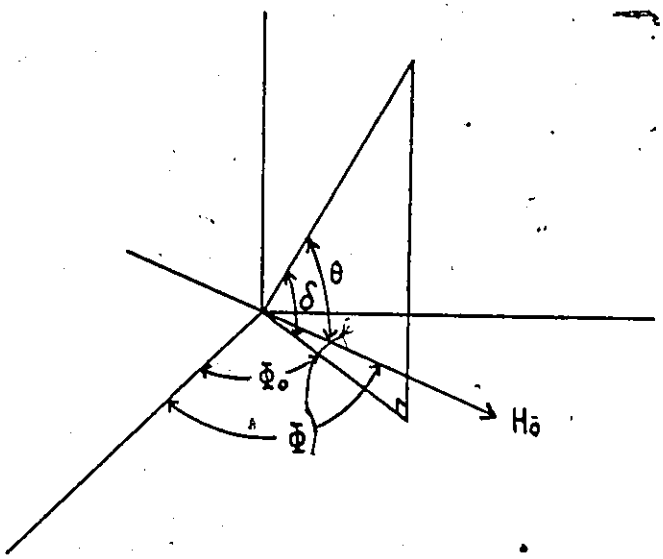

Fig. 4 Diagram defining various angles relating H_0 direction to crystal axes

Chapter II

EXPERIMENTAL

A. Single Crystal of $Er(C_2H_5SO_4)_3 \cdot 9H_2O$

The erbium ethylsulfate $Er(C_2H_5SO_4)_3 \cdot 9H_2O$ was made by adding stoichiometric amounts of a solution of barium ethylsulfate $Ba(C_2H_5SO_4)_2$ to an erbium sulfate solution. The barium ethylsulfate $Ba(C_2H_5SO_4)_2 \cdot 8H_2O$ was made by following the synthesis reported by Jean Grange.[15]

After the solution mixture was stirred for twenty-four hours barium sulfate was filtrated out. The filtrate was evaporated using a water condenser and vacuum pump with heating at temperatures from 30°C to 50°C; the temperature of the water vapour from erbium ethylsulfate solution was kept each time below 25°C.

When a considerable amount of solid was seen on the sides of the flask, the evaporation was stopped and these crystals were redissolved in the remaining unsaturated solution in the flask. The solution was then moved to the fume hood to evaporate slowly under a stream of nitrogen gas. After the solution was saturated, it was refrigerated around 8°C and crystallization begun. From the many small crystals that first formed, a few fine crystals were picked out and used as seeds.

Growth of a single crystal of $Nd(C_2H_5SO_4)_3 \cdot 9H_2O$ has been reported by R.A. Fisher[16] and we have followed his procedures. There are two kinds of shapes of crystals that can be used for seed crystals and these are shown in Fig. 5. Here a type A crystal was chosen

Figure 5

Crystal shapes of $Er(C_2H_5SO_4)_3 \cdot 9H_2O$

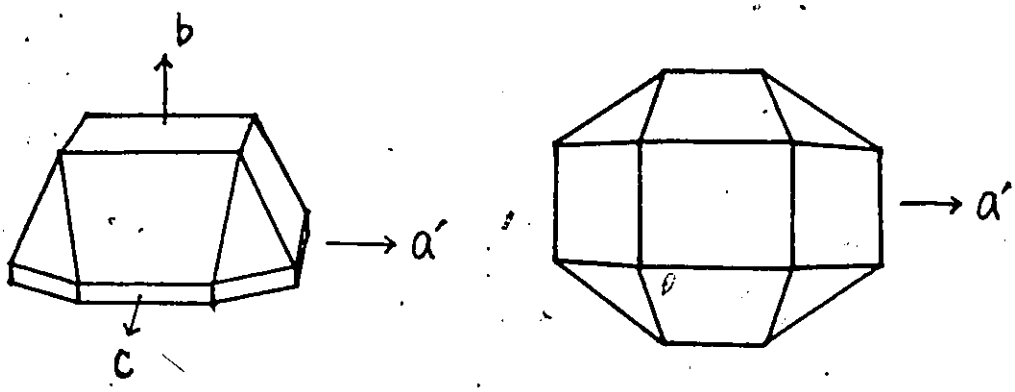

(A)

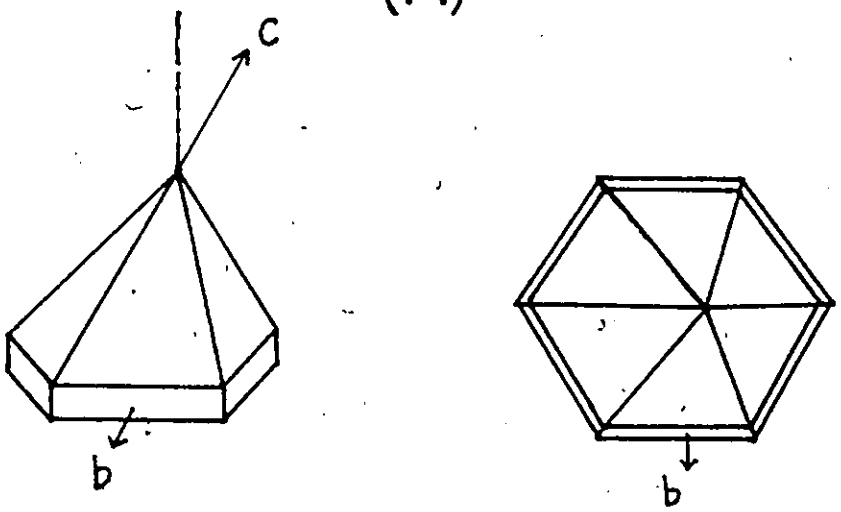

(B)

Figure 6

Crystal Structure of $Er(C_2H_5SO_4)_3 \cdot 9H_2O$

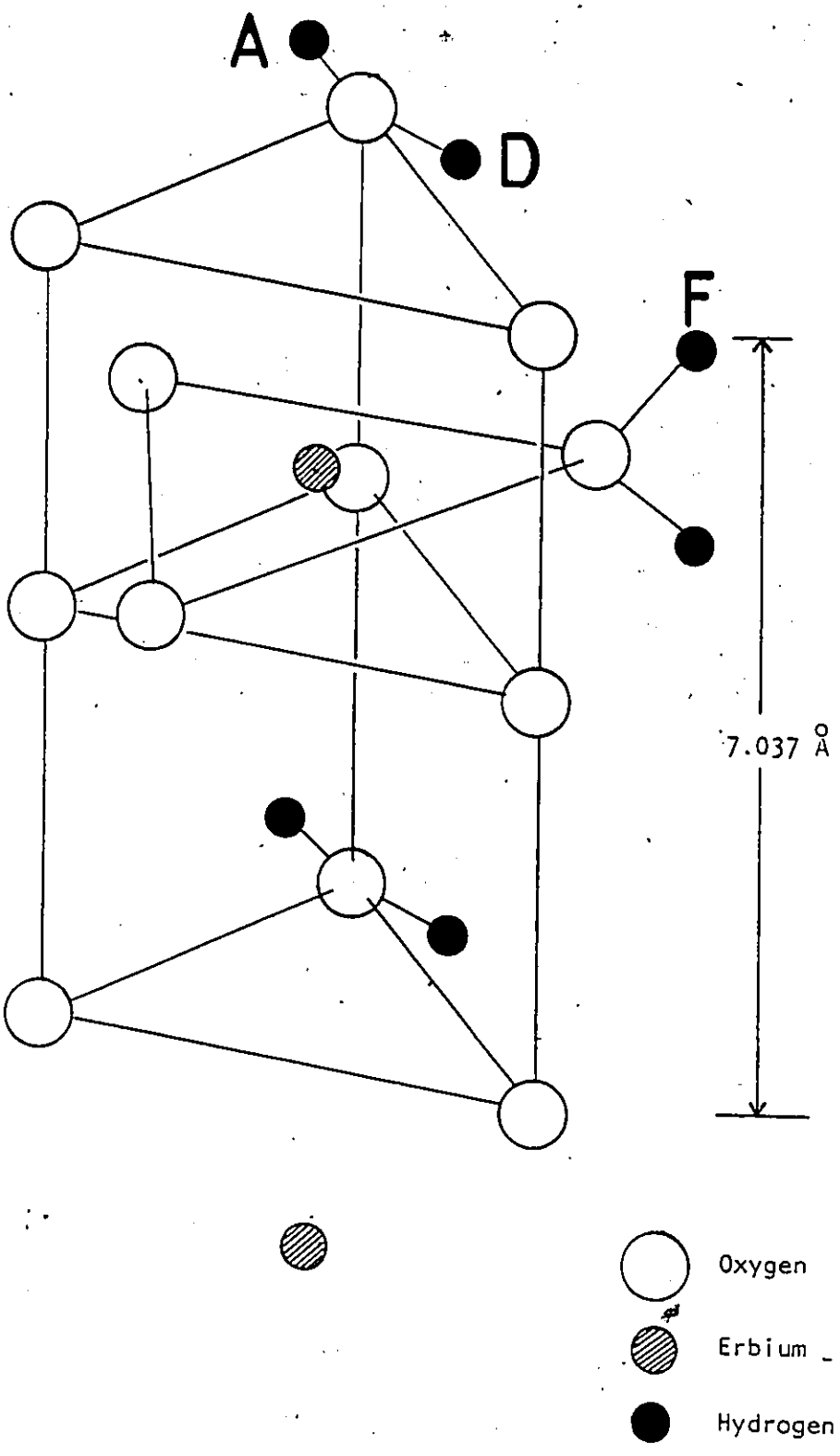
A
D
F
7.037 Å
Oxygen
Erbium
Hydrogen

because it gives the b crystallographic axis easily. The single crystal which we obtained was about 20 x 15 x 7 (mm). It was holed for the direction which is perpendicular to the crystallographic ac plane as shown in Fig. 5, and was ground to a sphere about 6 mm in diameter in the workshop of the University of Windsor. After the crystal was ground it was glued in a Teflon cube such that the direction of the hole in the crystal was parallel to the hole of the cube.

B. Crystal Structure

It is known that the crystal space group is P 63/m.[1] There are two magnetically equivalent Er sites per unit cell and the point symmetry at the metal ion is C_{3h}. The metal ion has nine water molecules as nearest neighbors; six form a trigonal prism above and below the mirror plane which contains the other three water oxygens and the metal ion.

For impurity rare-earth ethylsulfate $\cdot 9H_2O$ the water's hydrogens show five kinds of non-equivalent positions in symmetry; but for a single crystal of rare-earth ethylsulfate it is reduced to three kinds of non-equivalent positions.

The lattice constant of Er ethylsulfate $\cdot 9H_2O$ was given by Fitzwater and Rundle[2] as;

$$a = 13.915 \pm 0.001 \text{ Å}$$

From this value the c value calculated from the axial ratio which was given by Jaeger[17] is

$$c = 7.044 \text{ Å}$$

These values were used in the calculations of this paper.

All heavy atoms were found in the space group P 63/m and the distances between them are known, but hydrogen positions have not been determined yet for the Er ethylsulfate $\cdot 9H_2O$. It is possible that the hydrogen positions also conform to the same space group, that is P 63/m. The hydrogen positions of the Yb and Ho ethylsulfates $\cdot 9H_2O$ which were investigated by Albertsson et al.[3] and Hubbard et al.[4] are to be compared with the positions determined in this work.

The crystal structure is given in Figure 6.

C. NMR Technique and Operation

The NMR spectra were obtained using a broad line spectrometer constructed in our laboratory using mostly the components in our Varian E-12 ESR spectrometer to which were added an rf transmitter, a bridge, and an rf amplifier. The rf amplifier was set to 46 MHz and the magnetic field was set of 10830G and scanned in the range of 200 G.

The crystal was mounted inside a Teflon cube one face of which was glued to a support rod which was mounted perpendicular to the magnetic field and rotation plane. The teflon cube was inserted inside the rf coil which is attached to a glass tube and this whole part was covered by a Dewar tube as shown in Fig. 7.

The crystal will decompose when it is kept in the air for several weeks or sometimes several months, so that it was coated with glue. However, it was found that decomposition was rapidly promoted at room temperature by the radio frequency field. To prevent decomposition, spectra were run at temperatures between -22.5° and -28.5°C

Figure 7

Experimental arrangement of crystal

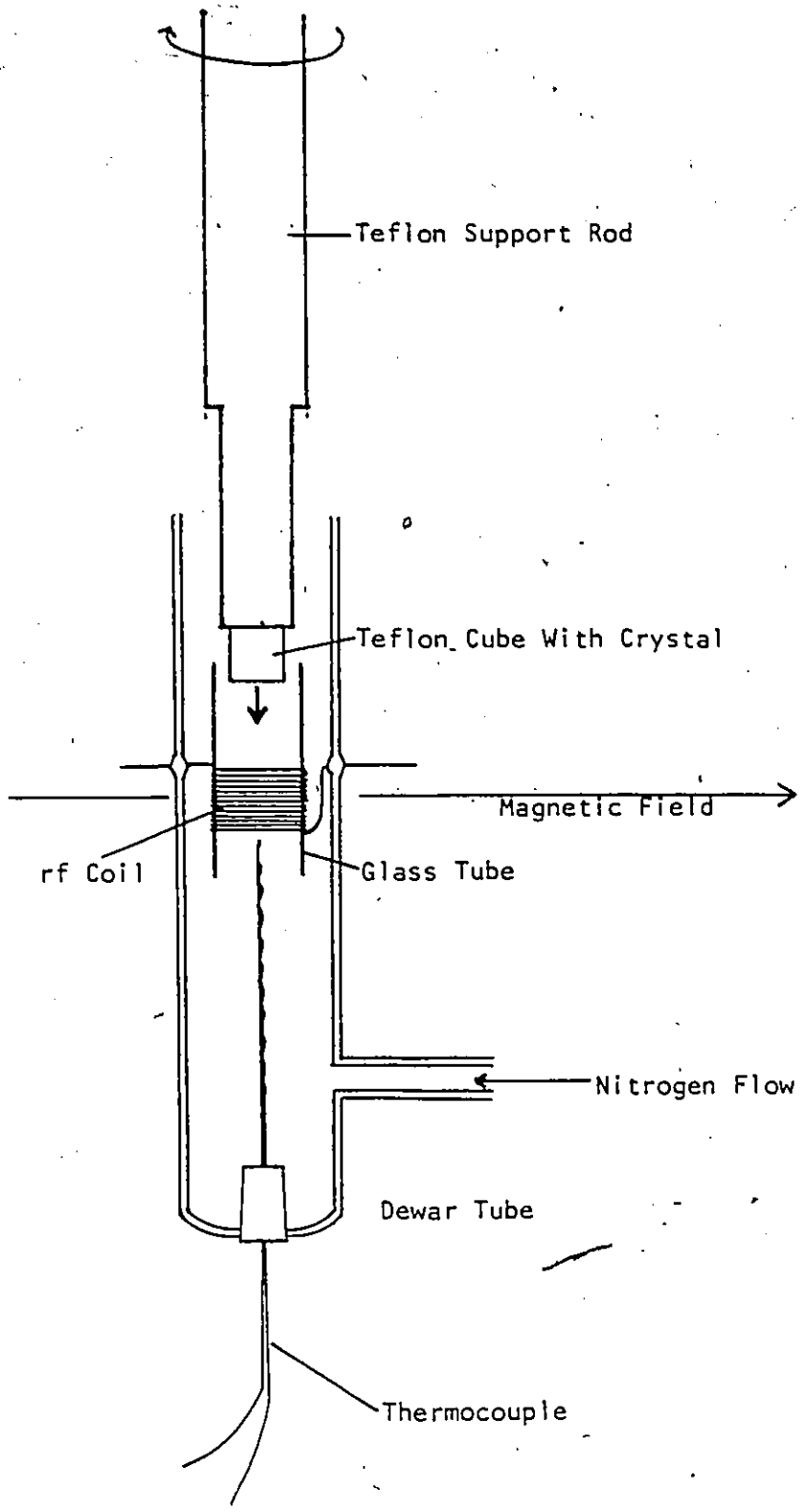
Teflon Support Rod
Teflon Cube With Crystal
Magnetic Field
rf Coil
Glass Tube
Nitrogen Flow
Dewar Tube
Thermocouple

obtained by nitrogen flowing in a Dewar tube, which was cooled by dry ice in an ethanol bath. After the temperature was measured, the thermocouple was taken out because of the noise it produces in the spectra, but the temperature was checked every two or three hours while spectra were run.

The NMR spectra were obtained for three mutually orthogonal planes by changing the face of the cube glued to the support rod. Spectra were taken every 5^{o} over a 180^{o} rotation of the crystal about the support rod. One of the three planes was approximately the ac plane of the crystal.

D. Analysis of Data and Results

One of the spectra is given in Fig. 8. The big center line came from protons in the glue which was used to mount the crystal in the Teflon cube. This line was used as the reference signal against which the paramagnetic shift was measured. For every line in each rotational plane the variation of shift was plotted as a function of laboratory rotation angle and is given in Fig. 9. The laboratory coordinates were taken to be the intersection of the three orthogonal rotational planes. These experimental points are fitted by a least-squares program to the equation.

$$\Delta H = A + B \cos 2\omega + C \sin 2\omega \qquad \{26\}$$

Eq. (26) is derived in Appendix A. The coefficients of this equation for each plane give parameters of the $\bar{a}$ tensor. In the experiment eleven sets of lines could be identified well enough to give eleven $\bar{a}$ tensors. These tensors were diagonalized. A diagonalized tensor can be divided into two tensors,

$$(\bar{a})^D = (\bar{a})^S + (\bar{a})^A \quad \{27\}$$

where $(\bar{a})^S$ is an isotropic tensor and $(\bar{a})^A$ is a traceless tensor. The values of the eleven sets are given in Table 1. For all eleven sets the isotropic shift is small and within experimental error can be taken to be zero.

The lines in Fig. 9 show characteristic pairs of lines. This splitting is due to the nuclear-nuclear dipolar interaction. For each pair the nuclear-nuclear dipolar interaction term was calculated and these were also diagonalized. For F sites the unique principal axis of the nuclear-nuclear dipolar interaction can be considered to be the c axis. Therefore, the c axis was located in the plane which was known to be the ac plane, from the lines' relations and the principal axes of the nuclear-nuclear dipolar interaction.

On the other hand, as shown in Appendix B, the multiplication of transformation matrices used to diagonalize two $\bar{a}$ tensors belonging to equivalent hydrogen sites will give the transformation matrix of the symmetry operation relating the two sites in laboratory frame. These transformation matrices of symmetry operations were calculated for each pair of lines and from these transformation matrices, the orientation of the c axis was calculated in the laboratory frame using the equations which are shown in Appendix C. The c axis agreed reasonably with the one obtained from the nuclear-nuclear dipolar interaction term. The transformation matrices for all operations of C_{3h} were calculated using the equations in Appendix C. Using two pairs of experimental lines in the three rotations these transformation matrices were used to predict all other lines in three

rotational planes belonging to equivalent sites in the crystal. These transformed lines were compared to the experimental points. Adjustments were made in the orientation of the c axis and assignment of points to lines until consistent agreement was obtained. Lines transformed in this manner are shown in Fig. 10. In this manner the best orientation of the c axis, best values of the experimental shift tensors, and the identification of which lines belong to which crystal sites were obtained.

Figure 8

First derivative of NMR absorption spectrum at 46.5 MHz for ^1H in a single crystal of $Er(C_2H_5SO_4)_3 \cdot 9H_2O$. The big centre line came from protons in the glue.

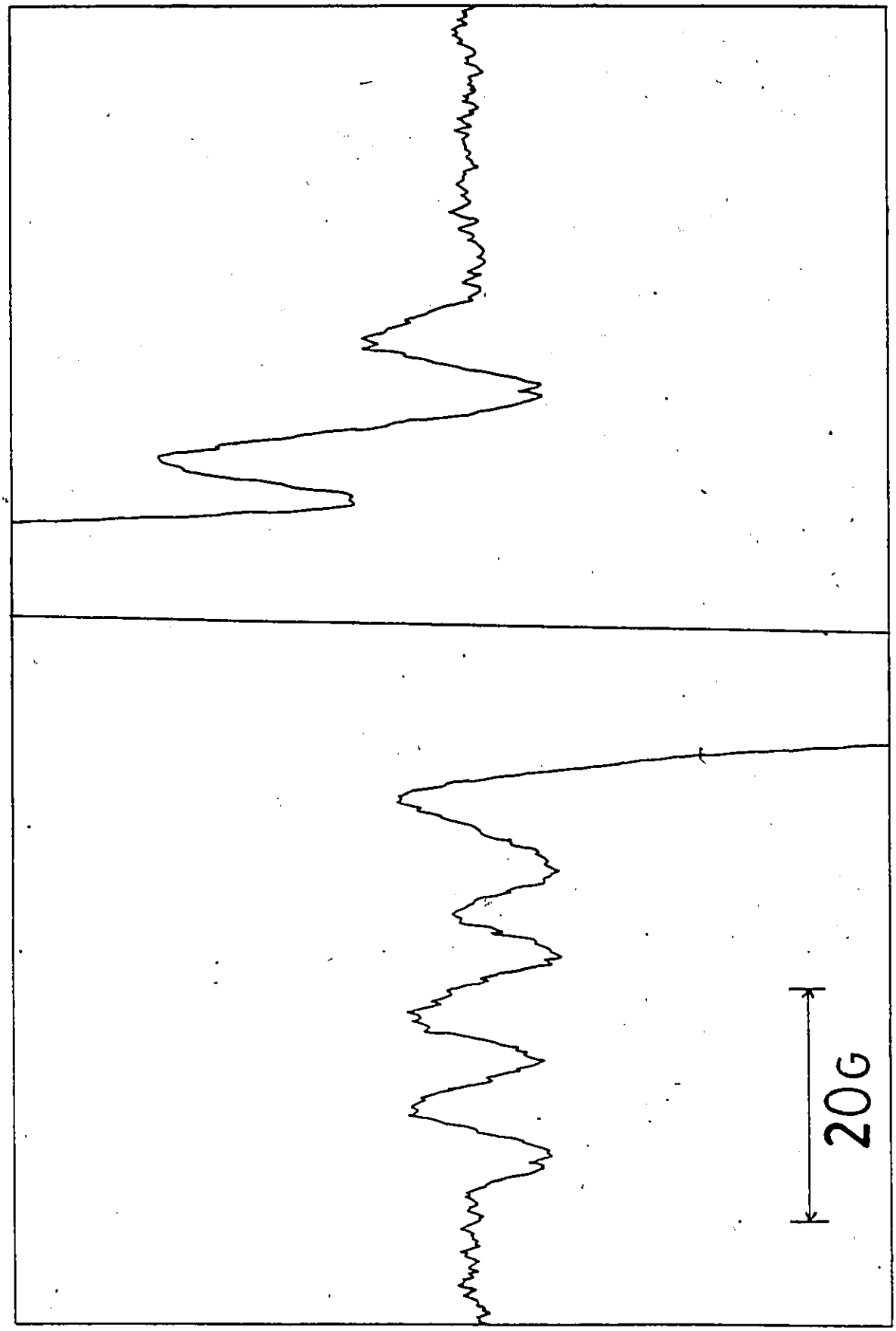
20G

Figure 9

Variation of resonance positions of proton lines of $Er(C_2H_5SO_4)_3 \cdot 9H_2O$ for rotation of crystal about an axis perpendicular to magnetic field. Points are experimental positions and the solid lines are least square-fitted curves from Eq.(26).

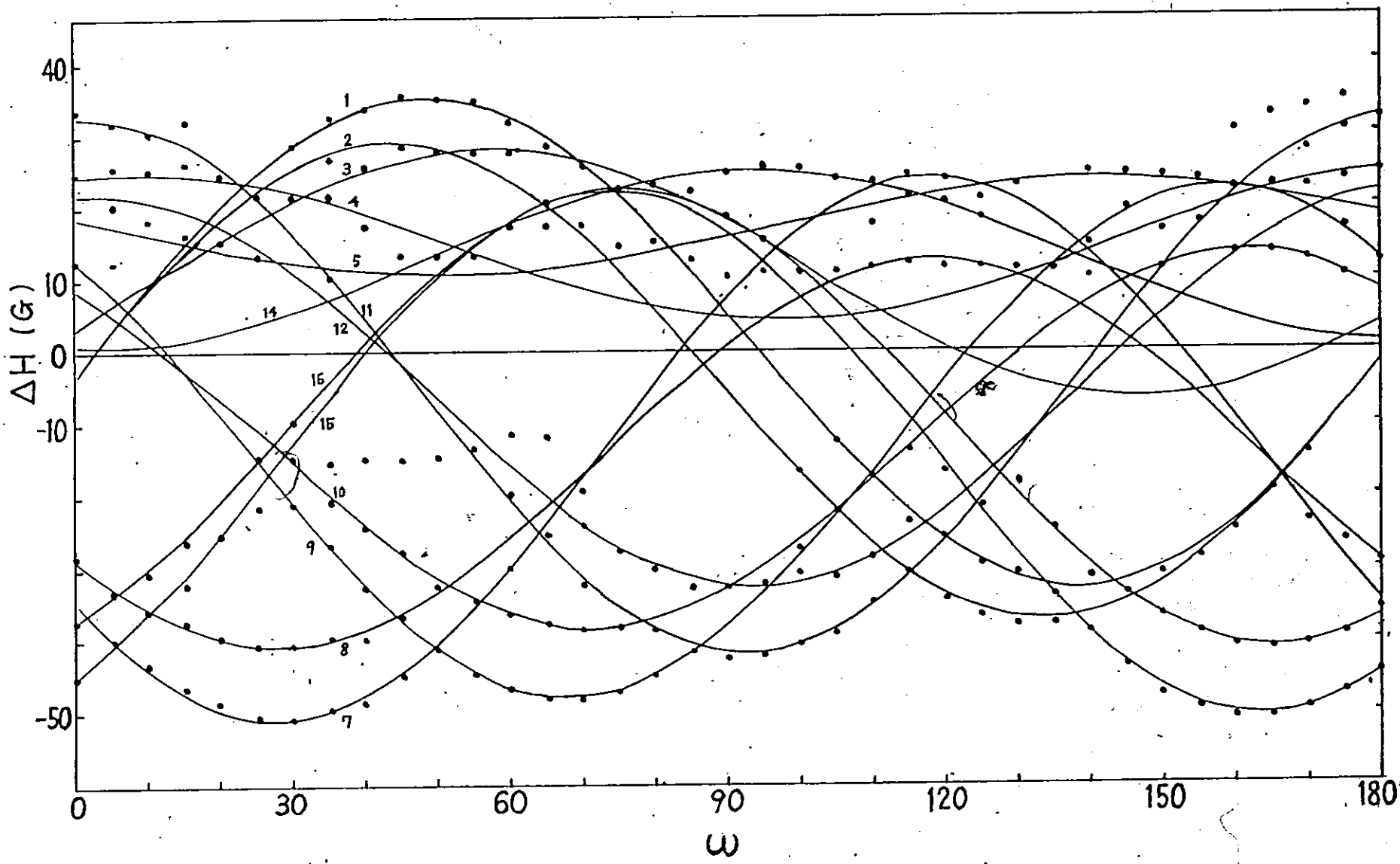
40
10
0
-10
-50
ΔH (G)
0
30
60
90
120
150
180°
ω
1
2
3
4
5
14
11
12
16
15
10
9
8
7

Figure 10

The experimental resonance positions and calculated lines using the transformation matrices for all operators of C_{3h} computed from the c axis by the way shown in Appendix C. The broken lines are original lines which came from 15, 16, 7, and 8 of the least square-fitted lines in Figure 9. All solid lines were obtained by transformation from the lines 15, 16, 7, and 8 and show good agreement with the least square-fitted lines in Figure 9. In this manner all least square-fitted lines were classified to each site. The identification of the lines and the symmetry operator which exists between lines one of which is 15 or 16 or 7 or 8 are given in Table 1.

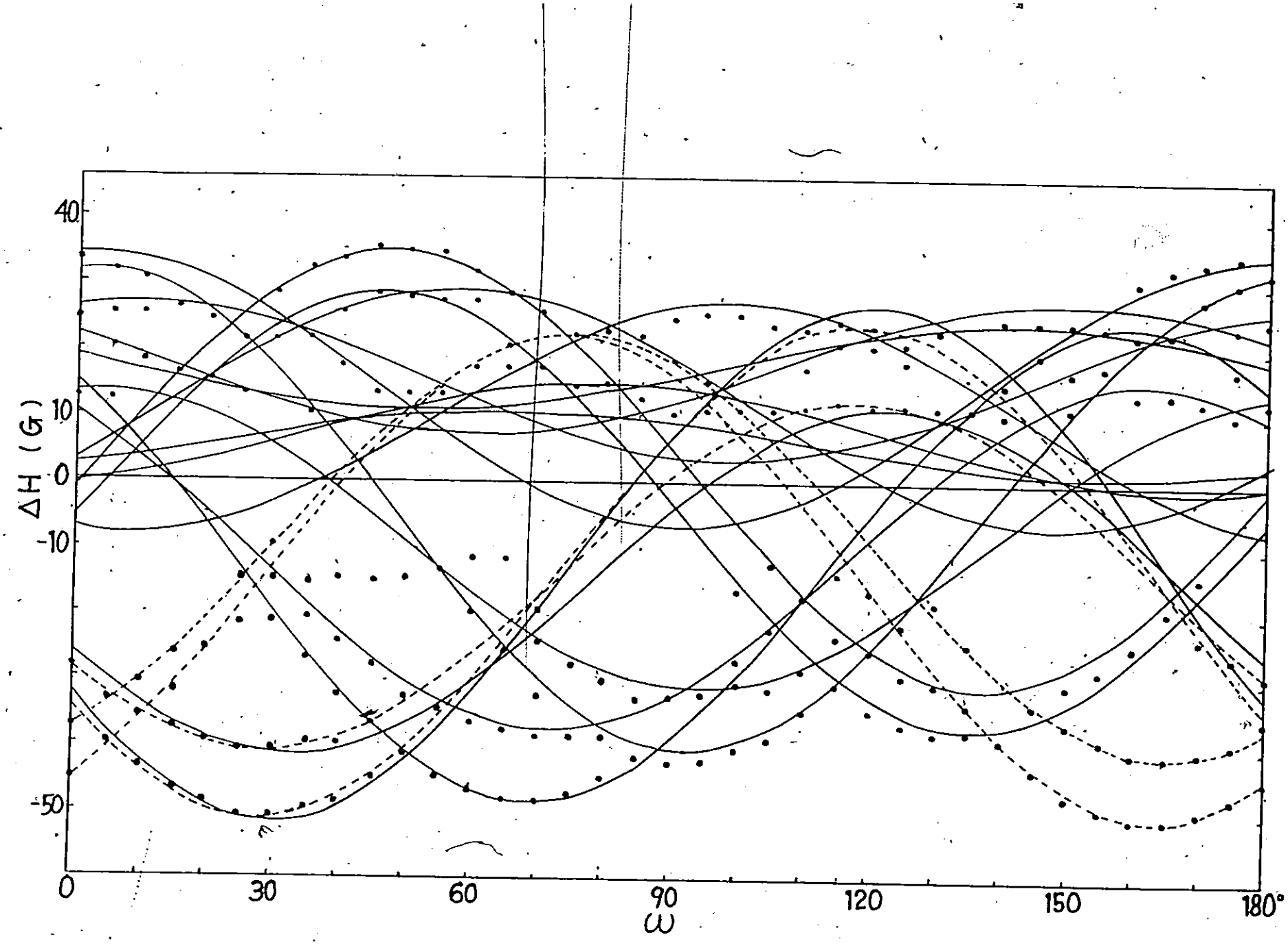
40
10
0
-10
-50
ΔH (G)
0
30
60
90
120
150
180°
ω

Table 1

PRINCIPAL VALUES OF SHIFT TENSOR FOR $Er(C_2H_5SO_4)_3 \cdot 9H_2O$

Values are given in units of 10^{-3}.

Lines	Site	Symmetry Operator	Isotropic Part	Principal Values	H-H Dipolar Interaction
1	A,D	$C_3 + \sigma$	0.02	$\begin{bmatrix} -4.19 \\ 3.16 \\ 1.04 \end{bmatrix}$	$\begin{bmatrix} -0.84 \\ 0.32 \\ 0.52 \end{bmatrix}$
2	A,D	$C_3 + \sigma$	0.02	$\begin{bmatrix} -4.94 \\ 3.09 \\ 1.85 \end{bmatrix}$	
3	A,D	$C_3^2 + \sigma$	0.01	$\begin{bmatrix} -4.94 \\ 2.91 \\ 2.03 \end{bmatrix}$	
6*	A,D	$C_3^2 + \sigma$	0.01	$\begin{bmatrix} -3.85 \\ 3.01 \\ 1.84 \end{bmatrix}$	
9	A,D	σ	0.02	$\begin{bmatrix} -4.85 \\ 3.01 \\ 1.84 \end{bmatrix}$	
10	A,D	σ	0.02	$\begin{bmatrix} -3.98 \\ 3.09 \\ 0.89 \end{bmatrix}$	

Table 1 (Continued)

Values are given in units of 10^{-3}.

Lines	Site	Symmetry Operator	Isotropic Part	Principal Values	H-H Dipolar Interaction
11*	A,D	C_3^2	0.02	$\begin{pmatrix} -5.01 \\ 3.04 \\ 1.97 \end{pmatrix}$	
12*	A,D	C_3^2	0.04	$\begin{pmatrix} -4.44 \\ 3.21 \\ 1.97 \end{pmatrix}$	
15	A,D	E	0.02	$\begin{pmatrix} -4.94 \\ 2.98 \\ 1.96 \end{pmatrix}$	$\begin{pmatrix} -0.84 \\ 0.34 \\ 0.49 \end{pmatrix}$
16	A,D	E	0.02	$\begin{pmatrix} -3.98 \\ 3.04 \\ 0.94 \end{pmatrix}$	
Average	A,D			$\begin{pmatrix} -4.91 \\ 3.00 \\ 1.92 \end{pmatrix}$	
				$\begin{pmatrix} -4.08 \\ 3.10 \\ 0.99 \end{pmatrix}$	

Table 1 (Continued)

Values are given in units of 10^{-3}.

Lines	Site	Symmetry Operator	Isotropic Part	Principal Values	H-H Dipolar Interaction
4	F	C_3^2 $C_3^2 + \sigma$	0.01	$\begin{bmatrix} -3.87 \\ 3.07 \\ 0.80 \end{bmatrix}$	$\begin{bmatrix} -0.83 \\ 0.40 \\ 0.43 \end{bmatrix}$
5	F	C_3^2 $C_3^2 + \sigma$	-0.01	$\begin{bmatrix} -4.68 \\ 2.53 \\ 2.15 \end{bmatrix}$	
7	F	E σ	-0.02	$\begin{bmatrix} -4.77 \\ 2.56 \\ 2.22 \end{bmatrix}$	$\begin{bmatrix} -0.82 \\ 0.37 \\ 0.46 \end{bmatrix}$
8	F	E σ	0.01	$\begin{bmatrix} 3.89 \\ 3.19 \\ 0.71 \end{bmatrix}$	
14	F	C_3 $C_3 + \sigma$	-0.02	$\begin{bmatrix} -4.69 \\ 2.50 \\ 2.19 \end{bmatrix}$	
Average	F			$\begin{bmatrix} -4.73 \\ 2.54 \\ 2.18 \end{bmatrix}$	
				$\begin{bmatrix} -3.88 \\ 3.13 \\ 0.75 \end{bmatrix}$	

Chapter III

DISCUSSION OF THE RESULTS

Nine pairs of lines were identified from the experimental points and this number is not enough for the eighteen proton sites of nine water molecules around Er^{3+} ion, for which eighteen pairs of lines are expected, and also the classification of these experimental lines showed unexpectedly that all experimental lines are of only two kinds. In fact, only one pair of lines is observed for each water molecule. It appears that some motional process is taking place which averages the shift tensor from the rare-earth ions for the two protons in the same water molecule but leaves the nuclear dipolar interaction between the proton pair intact. The explanation of the nature of this process awaits further study.

For each experimental pair of lines the shift tensor was diagonalized to obtain the three principal values. These were then compared to the principal values of shift tensors calculated from Eq. (20) using assumed coordinates for the H atoms and the values of the atomic susceptibility of $Er(C_2H_5SO_4)_3 \cdot 9H_2O$ obtained from the study of Cooke, Lazenby, and Leask.[18] This calculated tensor was obtained by averaging two tensors for the two protons in the water molecule term by term and then adding the nuclear dipolar tensor to them. The principal values are obtained by diagonalizing these tensors. The coordinates were varied until a good fit between the experimental and calculated values was obtained.

For the F site the H-H vector is parallel to the c axis so only two coordinates, the H-H distance and the Er-H distance needed

to be changed. For the H-H distance the experimental nuclear dipolar interaction already gave the value of 1.68 Å. For the A and D sites the nuclear dipolar interaction showed the angle between the H-H vector and the c axis to be about 60°. The calculation for the A and D sites first assumed this angle and further assumed the two O-H and Er-H distances were the same. Variation of the H-H distance and the Er-H distance failed, however, to give good agreement between calculated and experimental values. This assumption took the symmetry of the $Er(H_2O)_9^{3+}$ complex to be C_{3h}. Wolfe, et al. estimated the distances of A and D sites from Yb^{3+} to be 2.95 A and 3.03 A which would make the symmetry also C_{3h}. Further calculations of the shift tensor were made assuming the ratio of Er-H distances were the same as found by Wolfe, et al. Calculations were also done assuming the ratio to be the reciprocal of that given by Wolfe, et al.

The H-H distance and the H-O-H angle which gave the best agreement were 1.78 Å and 117.4° for the F site. For A and D sites the best agreement was obtained in the calculation with the reciprocal of the ratio of two distances which Wolfe, et al. gave, and the H-H distance and H-O-H angle were 1.78 Å and 119.4° . The distances of these protons from Er^{3+} ion were 3.19 Å for the F site, 3.06 Å for the A site and 2.98 Å for D site. For the F site the experimental error in the principal values is $\pm 0.1 \times 10^{-3}$, therefore the ranges of the angle and the distance are $112.6^{\circ} \leq$ H-O-H $\leq 122.2^{\circ}$ and 3.19 ± 0.03 Å. For the A and D site the ranges of angle and the distances are $117.3^{\circ} \leq$ H-O-H $\leq 121.4^{\circ}$ and 3.06 ± 0.02Å and 2.98 ± 0.02 Å with an experimental error of $\pm 0.15 \times 10^{-3}$ for the principal values.

The fractional coordinates of these positions are in Table 2 and the shift tensors are given in Table 3. The values which were obtained by McColl, et al.; Hubbard, et al.; and Albertsson, et al. are also in Table 2 and Table 3.

For the free water molecule the angle of H-O-H is 104.5° and the angles which were obtained here are bigger than this. The oxygens of sulfate, which are supposed to have hydrogen bondings with the hydrogens of F site are placed with the angle of 108.7° for $O(S)-O(H_2O)-O(S)$ which is greater than 104.5° but less than the angle found in this work. Neutron diffraction of the Ho compound by Hubbard, et al. also found a greater angle of 111.2°. Within experimental errors our angle agrees with that found from the neutron diffraction study. For the A and D sites the angle $O(S)-O(H_2O)-O(S)$ is 94.8°. Hubbard, et al. found the H-O-H angle to be 108.2° for these sites. The differences of our values could come from the uncertain ratio of the two Er-H distances. Since the F site shows a good agreement between the calculated values and the experimental values, the averaging procedure used for the two H atoms in H_2O must be reasonable and is not likely to be the reason for the much bigger angle of this work. If other ratios of two Er-H distances were tried, the principal values of the average of two tensors might agree with the experimental values at the smaller distance of H-H. It is difficult to believe that the two $O(H_2O)-H$ vectors are along the two $O(H_2O)-O(S)$ vectors and the angle of H-O-H is 94.8°, because this would make the water's electric dipole very far away from the $Er-O(H_2O)$ vector. Also the O(S)-O(S) vector is about 35° away from the c axis rather than the 60° which was obtained from the nuclear-nuclear dipolar

interaction. $O(H_2O)$-O(S) distance of the hydrogen A side is 2.73 Å and the other side is 2.85 Å which is bigger than 2.72 ± 0.04 Å of O-H···O normally found in hydrogen bonded solids as reported by Wallwork.[19] The angle between the $O(H_2O)$-O(S) vector and $O(H_2O)$-H_A site vector is about 13° from our calculations and the other H_D site is 29°. Therefore, hydrogen bonding is possible for the hydrogen of the A site to the sulfate oxygen, but not for the D site.

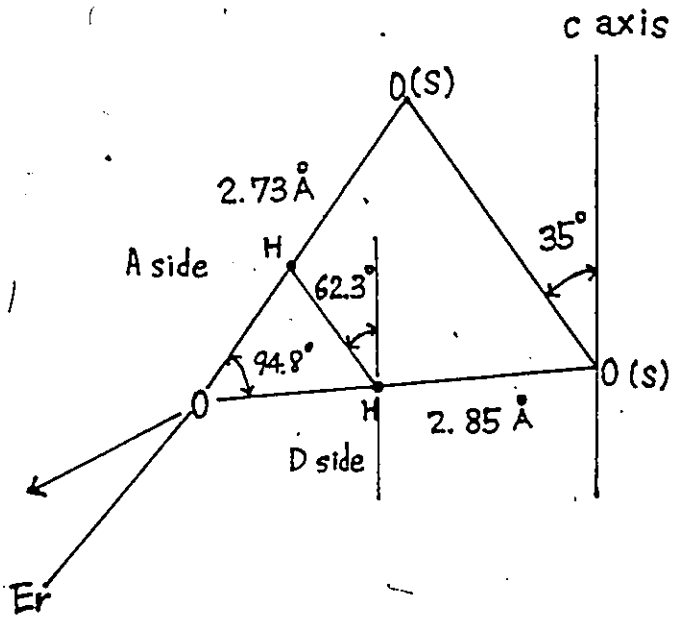

Figure 11 Relation when O-H vectors of the A and D sites are along O-O(S) vectors. This shows the difficulty that both sites have hydrogen bonding.

Table 2

Position of Hydrogens by Fractional Coordinates

$a = 13.911$ Å $\qquad c = 7.037$ Å [3]

		x	y	z
	Er	0.333	0.667	0.250
		0.667	0.333	0.750
McColl and Jeffries[20] *	A	0.223	0.497	-0.076
YES	D	0.140	0.529	-0.014
Theoretical Values	F	0.355	0.455	0.142
Hubbard, et al.[4]	A	0.235	0.507	-0.071
HoES	D	0.137	0.499	0.035
Neutron Diffraction	F	0.367	0.463	0.128
Albertsson, et al.[3] *	A	0.221	0.496	-0.075
PrES	D	0.155	0.508	0.018
	F	0.360	0.460	0.175
Albertsson, et al.[3] *	A	0.223	0.512	-0.062
YbES	D	0.145	0.503	0.038
	F	0.375	0.478	0.165
Our Calculated Coordinates	A	0.243	0.515	-0.097
ErES	D	0.132	0.522	0.019
	F	0.355	0.458	0.124

* These fractional coordinates were recalculated to get the same hydrogen positions Hubbard used.

Table 3 (a)

PRINCIPAL VALUES OF SHIFT TENSORS DUE ONLY TO Er^{3+} CALCULATED FROM PROTON POSITIONS DETERMINED BY OTHER METHODS

Values are given in units of 10^{-3}.
Values in upper row are isotropic part.

	A	D	F
McColl et al.[20]	0.10	-0.04	-0.08
YES	-4.58 2.63 1.94	-5.48 3.59 1.89	-4.76 2.84 1.92
Hubbard et al.[4]	0.12	-0.01	-0.07
HoES	-5.23 2.93 2.31	-5.80 3.56 2.24	-4.79 2.91 1.88
Albertsson et al.[3]	0.10	0.01	-0.09
PrES	-4.55 -2.63 1.92	-6.32 3.84 2.48	-5.14 3.07 2.08
Albertsson et al.[3]	-0.01	-0.10	-0.13
YbES	-5.64 3.22 2.42	-6.30 3.82 2.49	-5.79 3.48 2.31
Our Calculated Coordinates	0.14	0.00	-0.07
	-4.83 2.72 2.11	-5.88 3.73 2.14	-4.78 2.86 1.92

Table 3 (b)

PRINCIPAL VALUES OF Er^{3+} SHIFT TERM PLUS NUCLEAR-NUCLEAR DIPOLAR INTERACTION

Values are given in units of 10^{-3}.
Values in upper row are isotropic part.

	A	D	F
Our Calculation	-0.01	-4.12 3.24 0.88	-0.00	-3.95 3.20 0.75
	0.01	-4.82 3.02 1.82	0.00	-4.65 2.51 2.15
Experimental	0.02	-4.08 3.10 0.99	0.01	-3.88 3.13 0.75
	0.02	-4.91 3.00 1.92	-0.02	-4.73 2.54 2.18

Chapter IV

FURTHER INVESTIGATIONS

Some spectra were taken on the Brucker CXP-100 pulse spectrometer for the temperatures between 260°K and 160°K. As temperature decreased the spectral lines not only increased their shifts but also became broader and the number of lines increased. It is clear that there is some type of motional averaging depending on the temperature. It is not clear yet what the nature of this motional averaging is, but further study of the NMR in various orientations at lower temperatures for these crystals is definitely indicated.

APPENDIX A

When $\bar{a}$ is given as $\begin{bmatrix} a_{11} & a_{12} & a_{13} \\ a_{12} & a_{22} & a_{23} \\ a_{13} & a_{23} & a_{33} \end{bmatrix}$

$$\frac{\Delta H}{H_0} = \vec{h_0} \cdot \begin{bmatrix} a_{11} & a_{12} & a_{13} \\ a_{12} & a_{22} & a_{23} \\ a_{13} & a_{23} & a_{33} \end{bmatrix} \cdot \vec{h_0}$$

Since h_0 is a unit vector in the field direction, when it is on the laboratory xy plane it is given as

$$\vec{h_0} = \{\sin \omega, \cos \omega, 0\}$$

Therefore

$$\frac{\Delta H}{H_0} = \begin{bmatrix} \sin \omega, & \cos \omega, & 0 \end{bmatrix} \cdot \begin{bmatrix} a_{11} & a_{12} & a_{13} \\ a_{12} & a_{22} & a_{23} \\ a_{13} & a_{23} & a_{33} \end{bmatrix} \cdot \begin{bmatrix} \sin \omega \\ \cos \omega \\ 0 \end{bmatrix}$$

$$= \frac{a_{22} + a_{11}}{2} + \frac{a_{22} - a_{11}}{2} \cos 2\omega + a_{12} \sin 2\omega$$

where $\frac{a_{22} + a_{11}}{2} = A$ $\quad \frac{a_{22} - a_{11}}{2} = B$ $\quad a_{12} = C$

a_{11}, a_{12}, and a_{22} are given as

$$a_{22} = A+B$$

$$a_{11} = A-B$$

$$a_{12} = C$$

Similar calculations for the other planes give a_{33} and a_{13}.

APPENDIX B

When two $\bar{a}$ tensors which come from equivalent hydrogen sites are given as $\bar{a}_1$ and $\bar{a}_2$, these are written as

$$\frac{\Delta H}{H} = \vec{h}_0 \cdot \bar{a}_1 \cdot \vec{h}_0$$

$$\frac{\Delta H}{H} = \vec{h}_0 \cdot \bar{a}_2 \cdot \vec{h}_0$$

Diagonalized matrices, $\bar{a}_{1D}$ and $\bar{a}_{2D}$ are given by:

$$\bar{a}_{1D} = D_1 \cdot \bar{a}_1 \cdot \widetilde{D_1} \qquad \bar{a}_{2D} = D_2 \cdot \bar{a}_2 \cdot \widetilde{D_2}$$

where D is a three by three unitary matrix.

Since the diagonalized tensors which come from equivalent hydrogen sites are equal

$$\bar{a}_{1D} = \bar{a}_{2D}$$

Therefore $D_1 \cdot \bar{a}_1 \cdot \widetilde{D_1} = D_2 \cdot \bar{a}_2 \cdot \widetilde{D_2}$

$$\bar{a}_1 = \widetilde{D_1} D_2 \cdot \bar{a}_2 \widetilde{D_2} D_1$$

This can be written as

$$\bar{a}_1 = S \cdot \bar{a}_2 \cdot \widetilde{S}$$

where $S = \widetilde{D_1} \cdot D_2$ $\quad \widetilde{S} = \widetilde{\widetilde{D_1} \cdot D_2} = \widetilde{D_2} \cdot \widetilde{\widetilde{D_1}} = \widetilde{D_2} \cdot D_1$

In this work this S matrix is called a transformation matrix.

APPENDIX C

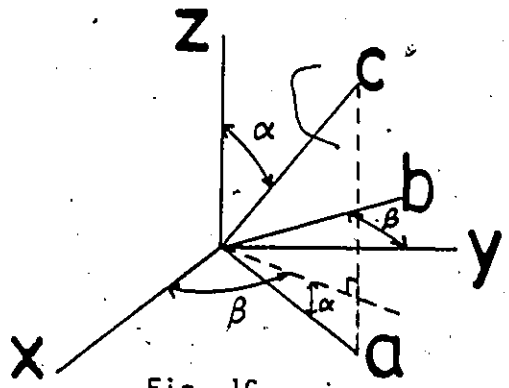

Fig. 1C

In Fig. 1C x,y,z are laboratory coordinates and a,b,c are crystallographic coordinates.

For vector H in coordinate system a,b,c

$$H_a = H_x\cos\alpha\cos\beta + H_y\cos\alpha\sin\beta - H_z\sin\alpha$$

$$H_b = -H_x\sin\beta + H_y\cos\beta$$

$$H_c = H_x\sin\alpha\cos\beta + H_y\sin\alpha\sin\beta + H_z\cos\alpha$$

When H vector is rotated about c axis by angle ω, the rotated vector H' is given by

$$H_a' = H_a\cos\omega + H_b\sin\omega$$

$$H_b' = -H_a\sin\omega + H_b\cos\omega$$

$$H_c' = H_c$$

When these are expressed by x,y,z coordinate system

$$H_x' = H_x\{\cos\omega\cos^2\alpha\cos^2\beta + \cos\omega\sin^2\beta + \sin^2\alpha\cos^2\beta\}$$
$$+ H_y\{(1-\cos\omega)\sin^2\alpha\sin\beta\cos\beta + \sin\omega\cos\alpha\}$$
$$+ H_z\{(1-\cos\omega)\sin\alpha\cos\alpha\cos\beta - \sin\omega\sin\alpha\sin\beta\}$$

$$H_y' = H_x\{(1-\cos\omega)\sin^2\alpha\sin\beta\cos\beta - \sin\omega\cos\alpha\}$$
$$+ H_y\{\cos\omega\cos^2\alpha\sin^2\beta + \cos\omega\cos^2\beta + \sin^2\alpha\sin^2\beta\}$$
$$+ H_z\{(1-\cos\omega)\sin\alpha\cos\alpha\sin\beta + \sin\omega\sin\alpha\cos\beta\}$$

APPENDIX C (Continued)

$$H_z' = H_x\{(1-\cos\omega)\sin\alpha\cos\alpha\cos\beta + \sin\omega\sin\alpha\sin\beta\}$$
$$+ H_y\{(1-\cos\omega)\sin\alpha\cos\alpha\sin\beta - \sin\omega\sin\alpha\cos\beta\}$$
$$+ H_z\{\cos\omega\sin^2\alpha + \cos^2\alpha\}$$

Therefore the transformation matrix for a rotation symmetry is given by.

$$\begin{bmatrix} S_{xx} & S_{xy} & S_{xz} \\ S_{yx} & S_{yy} & S_{yz} \\ S_{zx} & S_{zy} & S_{zz} \end{bmatrix}$$

where $S_{xx} = \cos\omega\cos^2\alpha\cos^2\beta + \cos\omega\sin^2\beta + \sin^2\alpha\cos^2\beta$

$S_{xy} = (1-\cos\omega)\sin^2\alpha\sin\beta\cos\beta + \sin\omega\cos\alpha$

$S_{xz} = (1-\cos\omega)\sin\alpha\cos\alpha\cos\beta - \sin\omega\sin\alpha\sin\beta$

$S_{yx} = (1-\cos\omega)\sin^2\alpha\sin\beta\cos\beta - \sin\omega\cos\alpha$

$S_{yy} = \cos\omega\cos^2\alpha\sin^2\beta + \cos\omega\cos^2\beta + \sin^2\alpha\sin^2\beta$

$S_{yz} = (1-\cos\omega)\sin\alpha\cos\alpha\sin\beta + \sin\omega\sin\alpha\cos\beta$

$S_{zx} = (1-\cos\omega)\sin\alpha\cos\alpha\cos\beta + \sin\omega\sin\alpha\sin\beta$

$S_{zy} = (1-\cos\omega)\sin\alpha\cos\alpha\sin\beta - \sin\omega\sin\alpha\cos\beta$

$S_{zz} = \cos\omega\sin^2\alpha + \cos^2\alpha$

Similar calculation for a rotation with reflection along c axis gives as following

$S_{xx} = \cos\omega\cos^2\alpha\cos^2\beta + \cos\omega\sin^2\beta - \sin^2\alpha\cos^2\beta$

$S_{xy} = -(1+\cos\omega)\sin^2\alpha\sin\beta\cos\beta + \sin\omega\cos\alpha$

$S_{xz} = -(1+\cos\omega)\sin\alpha\cos\alpha\cos\beta - \sin\omega\sin\alpha\sin\beta$

$S_{yx} = -(1+\cos\omega)\sin^2\alpha\sin\beta\cos\beta - \sin\omega\cos\alpha$

$S_{yy} = \cos\omega\cos^2\alpha\sin^2\beta + \cos\omega\cos^2\beta - \sin^2\alpha\sin^2\beta$

APPENDIX C (Continued)

$$S_{yz} = -(1+\cos\omega)\sin\alpha\cos\alpha\sin\beta + \sin\omega\sin\alpha\cos\beta$$

$$S_{zx} = -(1+\cos\omega)\sin\alpha\cos\alpha\cos\beta + \sin\omega\sin\alpha\sin\beta$$

$$S_{zy} = -(1+\cos\omega)\sin\alpha\cos\alpha\sin\beta - \sin\omega\sin\alpha\cos\beta$$

$$S_{zz} = \cos\omega\sin^2\alpha - \cos^2\alpha$$

REFERENCES

1. J.A.A. Ketelaar, Physica 4, 619 (1937)
2. D.R. Fitzwater and R.L. Rundle, Z Kristallogr. 112, 362 (1959)
3. J. Albertsson and I. Elding, Acta Cryst. 33, 1460 (1977)
4. C.R. Hubbard, C.O. Quicksall, and R.A. Jacobson, Acta Cryst. 30 2613 (1974)
5. G.E. Pake, J. Chem. Phys. 16, 327 (1948)
6. A.R. King, J.P. Wolfe, and R.L. Ballard, Phys. Rev. Lett. 28, 1099 (1972)
7. J.P. Wolfe, Phys. Rev. B. 16, 128 (1977)
8. R.G. Wheeler, F.M. Reames, and E.J. Watchel, J. Appl. Phys. 39, 919 (1968)
9. M.H.L. Pryce, Proc. Phys. Soc. (London), A63, 25 (1930)
10. A. Abragam and M.H.L. Pryce, Proc. Roy. Soc. (London), A205, 135 (1951)
11. R.J. Kurland and B.R. McGarvey, J. Mag. Res. 2, 286 (1970)
12. B.R. McGarvey, J. Chem. Phys. 58, 86 (1970)
13. J.H. Van Vleck, "The theory of Electric and Magnetic Susceptibilities," p. 131 (Oxford U.P., Oxford, England 1933)
14. A. Reuveni and B.R. McGarvey, J. Mag. Res. 29, 21 (1978)
15. J. Grange, Cahiers Phys. 15, 127 (1961)
16. R.A. Fisher, Rev. Sci. Instrum. 47, 1086 (1976)
17. F.M. Jaeger, Rec. Trav. Chim. 33, 343 (1914)
18. A.H. Cooke, R. Lazenby, and M.J.M. Leask, Proc. Phys. Soc., 85, 767 (1965)
19. S.C. Wallwork, Acta Cryst. 15, 758 (1962)
20. J.R. McColl and C.D. Jeffries, Phys. Rev. B. 1, 2917 (1970)

VITA AUCTORIS

Born: Kesennuma, Miyagi, JAPAN March 13, 1953

School:

Kesennuma Public Primary School
Kesennuma, Miyagi, JAPAN 1959-1965

Kesennuma Public Junior High School
Kesennuma, Miyagi, JAPAN 1965-1968

Miyagi Daini Joshi High School
Sendai, Miyagi, JAPAN 1968-1971

Yamagata University
Yamagata, Yamagata, JAPAN 1972-1976
Graduated with Bachelor of Science

University of Windsor
Windsor, Ontario, CANADA
As a Special Student 1976-1977
Graduate School 1977-1979